Available online at www.sciencedirect.com

SCIENCE DIRECT®

International Journal of Heat and Mass Transfer 47 (2004) 3649–3657

International Journal of HEAT and MASS TRANSFER

www.elsevier.com/locate/ijhmt

Interaction of interfacial convection and mass transfer effects in the system CO_2–water

B. Arendt, D. Dittmar, R. Eggers *

Department of Thermal Separation Processes, Process Engineering II, Heat and Mass Transfer, Technical University Hamburg-Harburg, Eissendorfer Strasse 38, 21071 Hamburg, Germany

Received 17 October 2003; received in revised form 13 April 2004

Abstract

The mass transfer of the system CO_2–water was measured up to a pressure of 360 bar at a temperature of 25 °C and the results were compared to empirical predictions. The influence of a surfactant on the mass transfer was investigated.

A Schlieren method and a three-mode magnetic suspension balance connected to an optical cell were used to analyse the mass transfer.

A good simulation of the experimental values was achieved by linear superposition of free convection and Marangoni convection. The surfactant enforces the Marangoni convection while the solubility of CO_2 stayed unaffected.

PACS: 42.79.Mt; 47.20.Ma; 68.05.–n; 06.30.Dr

Keywords: Convection; Natural convection; Mass transfer

---

1. Introduction

Although the phenomenon of interfacial convection has been known for over 150 years, only in recent time researchers have become more interested in this type of convection [1,2]. This interest arises from a changing view of engineers who abandon their generalized macroscopic view to turn to a more realistic comprehension of the different transport effects which are taking place at phase boundaries. Consequently, an improved calculation of mass transfer is desired.

Despite the fact that interfacial convection is superposed by free convection in most cases, in small and zero-gravity systems it is the dominant transport phenomenon. At the interface this kind of convection influences the mass transfer coefficient and so far it has not been studied to what extend it improves or decreases the mass transfer rate at elevated pressures. Thus, interfacial convection plays an important role in every system in which free surfaces occur, e.g. extraction or distillation, and for the design of the apparatus it is important to be able to describe and predict the influence on the mass transfer [1]. A clear distinction between the so-called Marangoni convection and free convection results from the nature and the direction of the driving forces relevant for mass transfer.

Marangoni convection is induced by differences in the interfacial tension along the phase boundary, whereas free convection is caused by density gradients perpendicular to the interface between the phase interface and the bulk phase. The mass transfer concerning the systems CO_2–water and CO_2–water containing a surfactant were investigated and compared with predictions based on empirical equations found by other researchers [3,4]. Furthermore, interfacial convection and free convection was visualised using a Schlieren technique. By this means a better understanding of the interaction of the two transport phenomena Marangoni

---

* Corresponding author. Tel.: +49-40-42878-3191; fax: +49-40-42878-2859.

E-mail address: r.eggers@tu-harburg.de (R. Eggers).

URL: http://www.tu-harburg.de/vt2.

0017-9310/$ - see front matter © 2004 Elsevier Ltd. All rights reserved.

doi:10.1016/j.ijheatmasstransfer.2004.04.011

Nomenclature

A	area
D	diffusion coefficient
g	gravity
L	characteristic length
m	mass
Ra	Rayleigh number $\frac{L^3 g(\rho(t \to \infty) - \rho(t))}{D\eta}$
Sh	Sherwood number $\frac{\beta L}{D}$
t	time
V	volume

Greek symbols

β	mass transfer coefficient
η	dynamic viscosity
σ	surface tension

Subscripts

A, 1	difference between the first measuring point and the zero point
A, 2	difference between the second measuring point and the zero point
ex	experimental
f	free convection
h	heavy phase
i	control variable
l	light phase
M	Marangoni convection
C	coupling
p	partial
ref	reference state
s	simulated
SK1	first sinker
SK2	second sinker
tot	total

convection and free convection is achieved and an a priori calculation of the mass transfer seems possible.

2. Materials and experimental set-up

The systems investigated in this work are CO_2 (Hydro) and water and CO_2 and water containing 4.75 wt.% of the surfactant Triton X-100 (SIGMA Chemical), which is a *t*-octylphenoxypolyethoxyethanol with a chain length from 9 to 10.

For both systems the changes of the water density with time due to the dissolution of CO_2 are measured at different pressures. The measurements were performed, using a three-mode suspension balance, which is a combination of a precision balance (Mettler AT 261 Delta Range), a heatable magnetic coupling (Rubotherm) and an optical cell (Sitec).

The combination of the magnetic suspension balance with an optical arrangement for the Schlieren method, which is described in detail in [5,6], allows the measurement of the densities and the visualisation of the mass transfer simultaneously. Furthermore, the Schlieren pictures are used to measure the changes in volume.

The pictures produced, using the Schlieren method, are recorded and transferred to a computer. From these pictures the change in volume is evaluated with a computer programme, which is described in detail elsewhere [7]. The complete experimental apparatus is shown in Fig. 1.

The experiments were carried out at a temperature of 25 °C and pressures between 80 and 360 bar, raising the pressure in 40 bar steps.

2.1. Density measurement

As mentioned above the density measurements are performed by a three-mode magnetic suspension balance.

In the first mode or zero point position only the permanent magnet system is kept in suspension (Fig. 2, right upper corner). Here the balance is tarred, which means that all results are differences between either the first or the second measuring point and the zero point.

In order to reach the first measuring point the permanent magnet is lifted by the electric magnet. Now the first sinker is kept in suspension while the second sinker stays on its seat (Fig. 2, bottom right corner). Then the permanent magnet is lifted a bit further to reach the second measuring point which means that both sinkers are kept in suspension (Fig. 2, centre). The exact function of the control system is described in [8–10]. According to Archimedes' law it is possible to calculate the densities in the upper (light phase) and in the lower (heavy phase) part of the optical cell (Fig. 2). Using a balance of forces for both sinkers, the densities can be estimated by the following equations:

$$\begin{aligned}\rho_h(t) &= \frac{m_{SK1} + m_C - m_{A,1}(t) - \rho_l(t)V_C}{V_{SK1}},\\ \rho_l(t) &= \frac{m_{SK2} + m_{A,1}(t) - m_{A,2}(t)}{V_{SK2}},\end{aligned} \tag{1}$$

where ρ signifies the density, m the mass and V the volume. The index C symbolizes the load coupling, SK1 the first sinker, which is located in the heavy phase, and SK2 the second sinker, which is located in the light phase. $m_{A,1}$ and $m_{A,2}$ stand for the difference between the

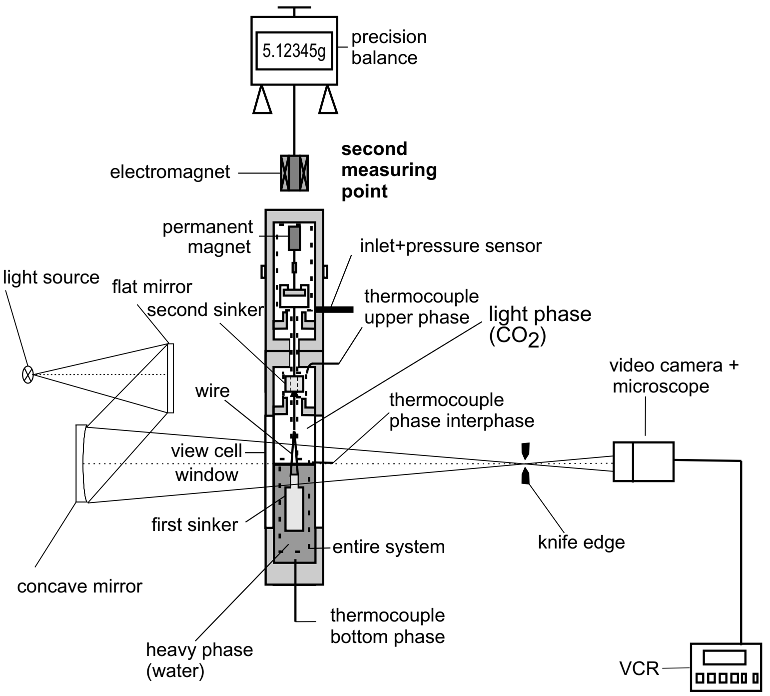

Fig. 1. Experimental apparatus.

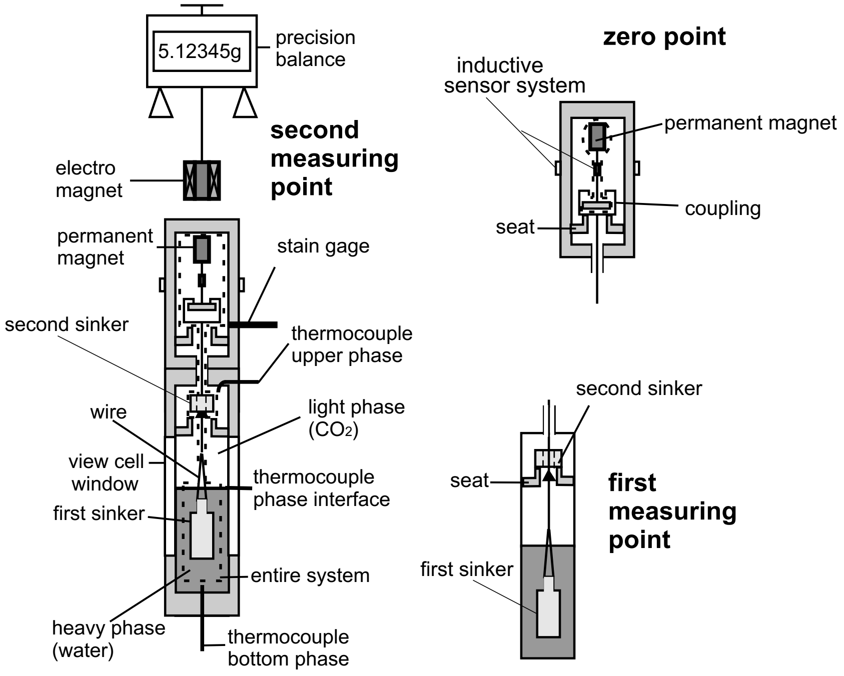

Fig. 2. Three-mode magnetic suspension balance.

mass measured in the first measuring point and in the second measuring point and the mass measured in the zero point, respectively. The mass and the volume of the sinker and the load coupling are determined by a calibration measurement with a fluid of known density [7]. The transferred mass of carbon dioxide is calculated according to the equation given below:

$$\rho_{\mathrm{l,p}}(t) = \frac{\rho_{\mathrm{h}}(t)V(t) - \rho_0 V_0}{V(t)},$$
$$m_{\mathrm{ex}}(t) = \rho_{\mathrm{l,p}}(t)V(t). \qquad (2)$$

Afterwards, the experimental results are compared to simulated masses. The procedure of the simulation is described in the following section in detail.

2.2. Simulated mass transfer

Mass transfer across plane quiescent phase boundaries in fluid–fluid systems consists of two different transport phenomena, which are free convection and interfacial convection. These mechanisms were considered separately in this work.

Free convection appears due to local differences in density and comprises the diffusional transport. In order to describe the transport by free convection empirical correlations of the Sherwood number and the Rayleigh number have been found. In this work the transport by free convection is described by a Sherwood equation for a plate cooled from below [3]:

$$Sh = 0.15Ra^{\frac{1}{3}}. \qquad (3)$$

In this case the Rayleigh number is defined as

$$Ra = \frac{L^3 g(\rho(t \to \infty) - \rho(t))}{D\eta}. \qquad (4)$$

L is the characteristic length, g the acceleration due to gravity, D the diffusion coefficient and η the dynamic viscosity. The mass transfer coefficient due to free convection can be calculated from equations (3) and (4) as follows:

$$\beta_{\mathrm{f}} = \frac{ShD}{L}. \qquad (5)$$

The interfacial convection or the so-called Marangoni convection arises from inhomogeneities in the interfacial tension at the phase interface. Correlating several systems, an equation for the prediction of the mass transfer coefficient due to Marangoni convection for a plane interface has been found by Hozawa et. al. [4]. Surfactants and elevated pressures were not considered in their equation. In this work the equation found by Hozawa [4] has been adapted in the following way:

$$\beta_{\mathrm{M}} = \sqrt{\frac{D}{\pi t}}\frac{\sigma_{\mathrm{ref}}}{\sigma}. \qquad (6)$$

In the equation above t symbolizes the time and σ the interfacial tension. The reference interfacial tension σ_{ref} depends on the contemplated system. Two separate cases are considered:

(1) system without surface active substance,
(2) system containing surfactant.

In case of the surfactant free system the reference interfacial tension is the surface tension of pure water at 1 bar and 25 °C, which is 72 mN/m. Eq. (6) adopts the original form found by Hozawa [4].

Since the original equation does not apply for systems containing surfactants and since the experimental results were not represented very accurately, using the original equation (see Fig. 3), the equation had to be changed, which leads to the second case. Considering this case the reference interfacial tension is the surface tension of water containing 4.75 wt.% tenside at 1 bar and 25 °C. The resulting value is 31.5 mN/m.

To calculate the mass of the carbon dioxide, which is transferred during a time interval between t_{i-1} and t_i, the mass transfer coefficient for the free convection is calculated. For that purpose the Rayleigh number is computed. The driving force is assumed to be the density difference between the actually measured density and the density at equilibrium. It is supposed that the phase interface remains at equilibrium conditions during the entire experiment. Having calculated the Rayleigh number by Eq. (4), the Sherwood number is computed by Eq. (3), which is transformed afterwards into the mass transfer coefficient for free convection using Eq. (5). The mass transfer coefficient concerning the Marangoni convection is computed using Eq. (6) for the mean time between t_{i-1} and t_i. Knowing the mass transfer coefficients, the masses of carbon dioxide transferred due to free convection and Marangoni convection can be calculated separately for any time interval by

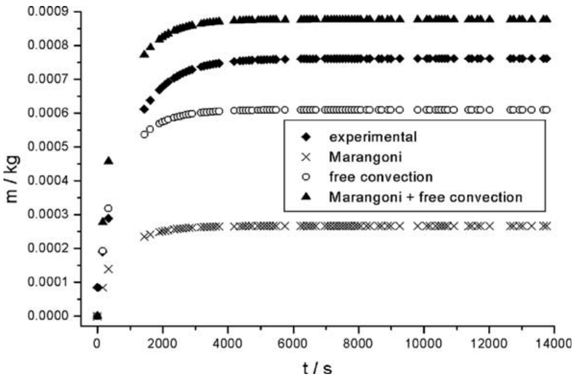

Fig. 3. Dependence of the transferred masses in the system CO_2–water containing 4.75 wt.% surfactant calculated with the original equation found by Hozawa [4] on time.

$$m_i(t_{i-1}, t_i) = \beta A(t_i - t_{i-1})\left(\rho_{1,\mathrm{p}}(t \rightarrow \infty) - \frac{\rho_{1,\mathrm{p,s}}(t_i) + \rho_{1,\mathrm{p,s}}(t_{i-1})}{2}\right). \tag{7}$$

In Eq. (7) β is the mass transfer coefficient, A the area through which the mass is transferred. t symbolises the time and $\rho_{1,\mathrm{p}}(t \rightarrow \infty)$ the partial density of CO_2 in water at equilibirum conditions. $\rho_{1,\mathrm{p,s}}(t_i)$ is a simulated partial density. In the first three time steps the simulated partial density is equated to the measured partial density. In each following time step the simulated partial density is calculated using Eq. (10). For the calculation of the total mass of the carbon dioxide, which is transferred into water, the simulated masses of the time intervals are summed up for the free convection and Marangoni convection:

$$m(t_i) = \sum_{i=1}^{n} m_i. \tag{8}$$

In the end the total transferred mass is calculated by

$$m_{\mathrm{tot}}(t_i) = m_{\mathrm{f}}(t_i) + m_{\mathrm{M}}(t_i). \tag{9}$$

The simulated partial density is calculated by the equation

$$\rho_{1,\mathrm{p,s}}(t_i) = \frac{m_{\mathrm{tot}}(t_{i-1})}{V(t_i)}. \tag{10}$$

2.3. Classification of the Schlieren

The detected Schlieren were classified according to these groups [11] (see also Fig. 4):

1. diverging flow: flow diverging at the surface and converging at the bottom,
2. plume density-driven convection,
3. interfacial turbulence: e.g. chaotic cells or hook-like plumes,
4. stratification: horizontal layers of significantly different concentration are built up.

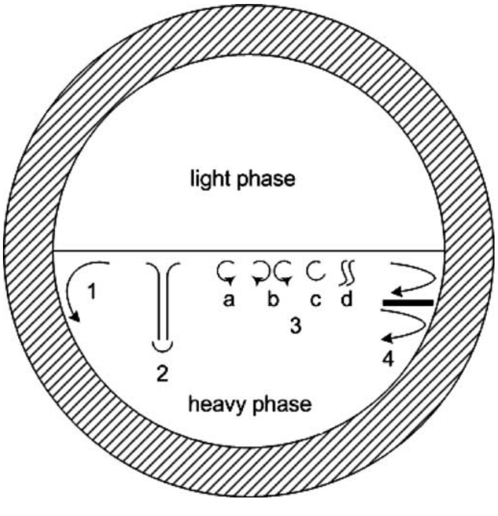

Fig. 4. Convection pattern classes [11].

3. Results and discussion

3.1. Convection patterns

The Sternling and Scriven analysis [12] of the system CO_2–water up-front stated that no interfacial instabilities are to be expected. Nevertheless, both systems, the system CO_2–water as well as the CO_2–water with tenside, show convective flow patterns including interfacial convection. Reasons why the analysis of Sternling and Scriven [12] does not predict correctly lies in the fact that the majority of the assumptions are not fulfilled. These unfulfilled assumptions are:

1. semi-infinite, immiscible phases,
2. fluid properties which are independent of the transferred substance,
3. steady-state mass transfer,
4. thermal equilibrium at the beginning of an experiment due to the heat of solution.

In Fig. 5 the Schlieren detected in the systems CO_2–water and CO_2–water mixed with tenside are exemplarily shown. The upper phase is CO_2 and the lower phase is water.

Classifying the Schlieren in the lower phase shows that in both systems the same types of Schlieren occur: the diverging flow, plumes and interfacial turbulence of the hook-like plume type. The amount of Schlieren and their velocity decrease with time because the systems turn towards equilibrium.

In the system CO_2–water the Schlieren can only be observed at a pressure of 80 bar. The other pressure levels did not show any Schlieren. In contrast to this observation interfacial convection could be seen at all pressure levels in the system containing tenside. Another difference to the pure water system is that a larger amount of smaller, more chaotic Schlieren was observed. One possible explanation of this behaviour is that the tenside influences the optical properties of the mixture making it possible to see smaller density gradients. Larger density gradients are another possible cause of the fact that Schlieren can also be detected at higher pressures. Even an increase in Marangoni convection due to the surfactant could be a reason. This assumption is in agreement with the observation that the equilibrium is reached earlier in the system

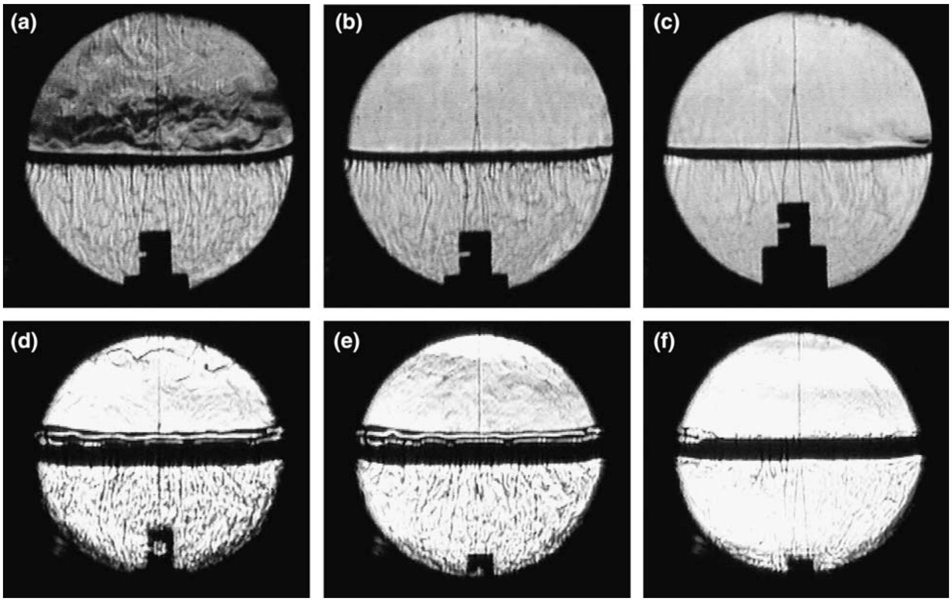

Fig. 5. Schlieren patterns (a) CO_2–water after 2 min 2 s, (b) CO_2–water after 8 min 6 s, (c) CO_2–water after 34 min, (d) CO_2–water containing tenside after 2 min 12 s, (e) CO_2–water containing tenside after 8 min 6 s, (f) CO_2–water containing tenside after 32 min.

containing the surfactant than in the pure water system (see Fig. 6 in Section 3.2). Furthermore, the proportion of the mass transferred by Marangoni convection is lower in the latter system than in the former (compare Tables 1 and 2). Further conceivable explanations are the following:

1. Reducing the interfacial tension and hereby reducing the difference in interfacial tension between equilibrium and beginning of an experiment diminishes the energy needed to produce new surface area which makes it easier to create new surface area and, thus, leads to earlier and faster Schlieren.
2. Reducing the interfacial tension simplifies the diffusion of CO_2 into the water. This leads to a faster build-up of the density gradient again leading to earlier and faster Schlieren.

Both reasons also explain that the equilibrium of the system CO_2–water with tenside is reached earlier than in the other system (see Fig. 6 in Section 3.2).

3.2. Mass transfer

According to Eq. (1) for each pressure level the density is calculated from the weighing results. Fig. 6 exemplarily shows the results of the density measurement of the heavy phase for the two systems at a pressure of 80 bar and a temperature of 25 °C. As mentioned in Section 3.1 it can be seen that the equilibrium is reached earlier in the system CO_2–water containing tenside than in the system CO_2–water. Nevertheless, for every pressure level the density at equilibrium is about 0.2% higher in the system containing surfactant than in the pure water system. The slightly higher density is a

Table 1
Summary of the results concerning the mass transfer of CO_2 in the system CO_2–water

p, bar	Deviation $(m_M + m_f) - m_{ex}$, %	Contribution to mass transfer, %	
		m_M	m_f
79.07	−14.7/−2.3	16.38	83.62
120.96	−8.2/−4	60.19	39.81
159.38	−4.8/−0.5	53.24	46.76
200.23	−4.4/−1.6	55.92	44.08
239.42	−5/−1.4	78.74	21.26
280.38	−4/−0.2	68.65	31.45
321.76	−5/−0.6	70.85	29.15
363.44	−5.3/−2.3	97.49	2.51

Table 2
Summary of the results concerning the mass transfer of CO_2 in the system CO_2–water containing tenside calculated with $\sigma_{ref} = 31.5$ mN/m

p, bar	Deviation $(m_M + m_f) - m_{ex}$, %	Contribution to mass transfer, %	
		m_M	m_f
76.12	−17.8/−1.2	44.56	55.44
122.43	−5.8/−1.5	71.59	28.41
157.84	−4.5/−0.7	82.74	17.26
197.74	−2/−0.7	75.48	24.52
240.08	−4.2/−0.9	81.01	18.99
280.5	−3.1/−0.6	83.26	16.74
321.57	−3.8/−0.5	89.13	10.87

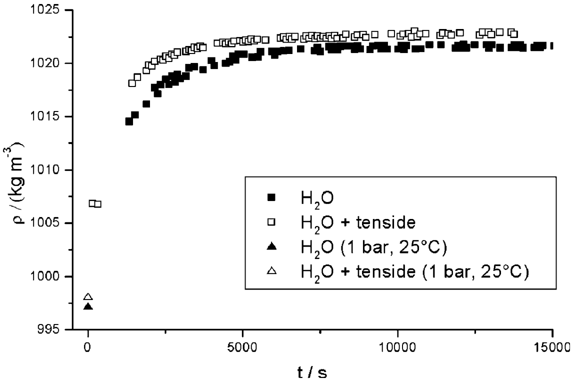

Fig. 6. Dependence of the densities of the systems CO_2–water and CO_2–water containing surfactant at 80 bar and 25 °C on time.

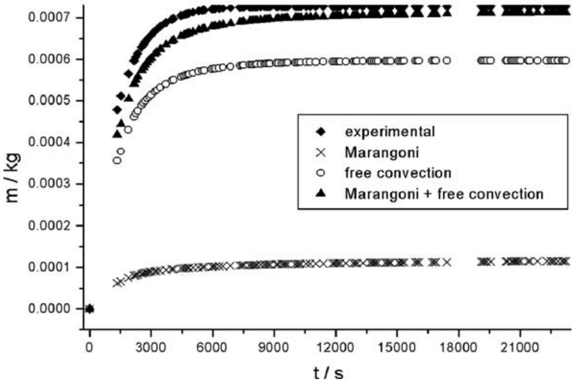

Fig. 7. Dependence of the transferred mass of the system CO_2–water at a pressure of 80 bar and a temperature of 25 °C on time.

sole consequence of the increase of the density due to the added amount of surfactant, because the solubility of CO_2 in water is not affected by the addition of the tenside, which is shown by the fact that the same amount of CO_2 is transferred in both systems.

The mass transported by free convection and Marangoni convection is calculated using Eqs. (7)–(10). The mass transfer coefficients due to Marangoni convection and free convection are estimated by Eq. (6) and equations (3)–(5), respectively.

For the system CO_2–water Fig. 7 shows a very good agreement of the experimental values and the values gained using the principle of linear superposition for the simulated values. The deviation lies in between −14.7% and −2.3%. Raising the pressure level, the agreement of the experimental values and the values according to the principle of linear superposition even improve with deviations between −8.2% and −0.2%.

Considering the different transport mechanisms separately at a pressure of 80 bar and a temperature of 25 °C, 83.62% of the total mass is transferred by free convection and 16.38% by Marangoni convection. However, with increasing pressure the proportion of free convection decreases while the one of Marangoni convection increases. The relative proportion of diffusion, which is accounted for in the description of the free convection by Sherwood correlation, increases with increasing pressure. The reason for the declining free convection lies in the increasing solubility of CO_2 in water with increasing pressure and that at the same time the effect of the solution of CO_2 in water on the density decreases. As a consequence of these circumstances the density increases only slightly leading to a lower driving force for free convection with increasing pressure. The results for the system CO_2–water are summarised in Table 1.

In Fig. 8 the development of the transferred mass with time is shown for the system CO_2–water containing 4.75 wt.% Triton X-100 at a pressure of 80 bar and 25 °C.

Fig. 8 shows that the calculated mass deviates −17.8% from the experimental mass at the beginning of the experiment. However, the deviation at the end of the experiment is much better reducing to only −1.2%. This observation verifies that by changing the reference state in Eq. (6) the quality of the agreement resembles the one

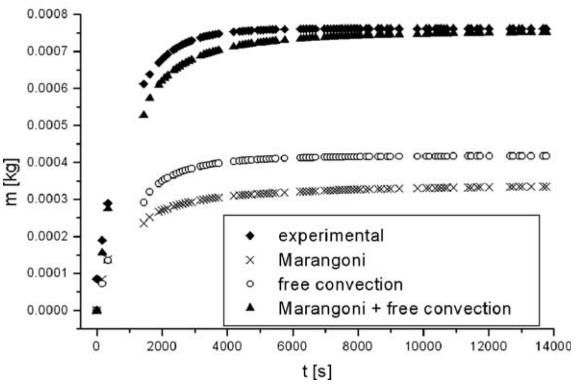

Fig. 8. Dependence of the transferred mass of the system CO_2–water containing surfactant calculated with $\sigma_{ref} = 31.5$ mN/m at a pressure of 80 bar and a temperature of 25 °C on time.

in the system CO_2–water and is much better than using the original equation found by Hozawa et al. [4] (compare Figs. 3 and 8). The agreement of the higher pressure levels is varying between −5.8% and −0.5% and therefore, as good as in the system CO_2–water.

Furthermore, the transport phenomena have also been considered separately for the system CO_2–water containing surfactant. At a pressure of 80 bar and a temperature of 25 °C 44.56% of the mass is transported by Marangoni convection and 55.44% by free convection. Again the proportion of Marangoni convection increases with increasing pressure while the fraction of free convection decreases. The proportion of Marangoni convection increases on a higher level compared to the system CO_2–water. The explanation for the decline of the free convection is the same as described for the system CO_2–water. The results for this system are summarised in Table 2.

4. Conclusion

Considering the experimental results it can be stated that the assumption of the principle of linear superposition for the two mass transfer mechanisms is valid for a plane interface. In case of the system containing surfactant the description of the Marangoni convection is insufficient if the standard equation found by Hozawa et. al. [4] is used. Changing the reference state seems to be a good and reasonable alternative, since it leads to an agreement of the experimental data and the calculated values of the same quality as in the system CO_2–water. The good agreement shows that the empirical equations used predict the experimental values with a sufficient accuracy. Moreover, the experiments indicate that the surfactant enforces Marangoni convection, as the proportion of the mass transferred by Marangoni convection is higher in the system containing the tenside. Additionally, more and apparently faster Schlieren can be seen at the interface and the equilibrium is reached earlier than in the pure water system. The density of the surfactant–water mixture is slightly higher due to the tenside than in the system with pure water, while the solubility of CO_2 stays unaffected.

Despite this good agreement, none of the results does show that the assumption of the linear superposition of the two mass transfer effects is appropriate in case of any other interface like droplets or spheres. The mass transfer across these surfaces is in the perspective of our further investigations.

Furthermore, for both systems convective patterns have been made visible, using a Schlieren method. The patters have been classified and the results agree with other studies.

Acknowledgements

The financial support by the German Research Community (DFG), project DFG EG 72/14, is gratefully acknowledged.

References

[1] J. Betz, Strömung und Wärmeübergang bei thermokapillarer Konvektion an Gasblasen, Herbert Utz Verlag Wissenschaft, München, 1997.

[2] S. Wolf, Phasengrenzkonvektionen beim Stoffübergang in Flüssig-Flüssig-Systemen, Reihe 3, Nr. 584, VDI Verlag, Düsseldorf, 1999.

[3] H.D. Baehr, K. Stephan, Heat and Mass Transfer, Springer, Berlin, Heidelberg, New York, 1998.

[4] M. Hozawa, N. Komatsu, N. Imaishi, K. Fujinawa, Interfacial turbulence during the physical absorption of carbon dioxid into non-aqueous solvents, J. Chem. Eng. Jpn. 17 (2) (1984) 173–179.

[5] F. Mayinger, O. Feldmann, Heat and Mass Transfer: Optical Measurement Techniques and Applications, Springer, Berlin, Heidelberg, New York, 2001.

[6] G.S. Settles, Schlieren and Shadowgraph Techniques: Visualizing Phenomena in Transparent Media, Springer, Berlin, Heidelberg, New York, 2001.

[7] A. Tegetmeier, D. Dittmar, A. Fredenhagen, R. Eggers, Density and volume of water and triglyceride mixtures in carbon dioxide, Chem. Eng. Process. 39 (2000) 399–405.

[8] A. Docter, H.-W. Lösch, W. Wagner, Entwicklung und Aufbau einer Anlage zur simultanen Messung der Viskosität und der Dichte fluider Stoffe, Fortschritt-Berichte der VDI-Zeitschriften, Reihe 3, Nr. 494, VDI-Verlag, Düsseldorf, 1997.

[9] H.-W. Lösch, Entwicklung und Aufbau von neuen Magnetschwebewaagen zur berührungsfreien Messung vertik-

aler Kräfte, Fortschritt-Berichte der VDI-Zeitschriften, Reihe 3, Nr. 138, VDI-Verlag, Düsseldorf, 1987.

[10] R. Kleinrahm, W. Wagner, Entwicklung und Aufbau einer Dichtemeßanlage zur Messung der Siede- und Taudichten reiner fluider Stoffe auf der gesamten Phasengrenzkurve, Fortschritt-Berichte der VDI-Zeitschriften, Reihe 3, Nr. 92, VDI-Verlag, Düsseldorf, 1984.

[11] A. Okhotsimskii, M. Hozawa, Schlieren visualization of natural convection in binary gas–liquid systems, Chem. Eng. Sci. 53 (14) (1998) 2547–2573.

[12] C.V. Sternling, L.E. Scriven, Interfacial turbulence: hydrodynamic instabilities and the Marangoni effect, AIChE J. 5 (1959) 514–523.